

The synergistic cooperation of NH \cdots O and CH \cdots O hydrogen bonds in the structures of three new phosphoric triamides

Anahid Saneei^a, Mehrdad Pourayoubi^{a,*}, Jerry P. Jasinski^b, Titus A. Jenny^c, Aurelien Crochet^d, Katharina M. Fromm^d, Amanda C. Keeley^b

^aDepartment of Chemistry, Faculty of Sciences, Ferdowsi University of Mashhad, Mashhad, Iran, Tel: +985138805535, Fax: +985138807153, P.O. Box: 9177948974

^bDepartment of Chemistry, Keene State College, 229 Main Street, Keene, NH 03435-2001, USA

^cDepartment of Chemistry, University of Fribourg, Rte du Musée 9 Ch-1700 Fribourg, Switzerland

^dFribourg Centre for Nanomaterial's, FriMat, University of Fribourg, Chemin du Musée 3, CH-1700 Fribourg, Switzerland

Email: pourayoubi@um.ac.ir

Supplemental Materials

Background of the Hirshfeld surface analysis

Historically, the Hirshfeld surface (HS) emerged from an effort to define the space occupied by a molecule in a crystal for the purpose of partitioning crystalline electron density into molecular fragments.^{ES1} Such a surface was named in honor of F. L. Hirshfeld, who introduced the “stockholder partitioning” scheme.^{ES2} Afterwards, it was realized that the Hirshfeld surfaces possessed a number of attributes that make them attractive for identification of intermolecular interactions in the context of crystal packing.^{ES3} In a Hirshfeld surface, the parameters d_e and d_i describe the distances from a point on the surface to the nearest nucleus outside and inside the

surface, respectively. The d_{norm} value is the sum of the normalised quantities of d_i and d_e by considering the van der Waals radius of atoms involved. This value graphically highlights the regions of the surface involved in a specific type of intermolecular contact by a colored scheme: red regions represent contacts shorter than the sum of van der Waals radii; white regions represent intermolecular distances close to van der Waals contacts and blue regions represent contacts longer than the sum of van der Waals radii.^{ES4} The fingerprint plots (FPs) are introduced as the two-dimensional representations of the information provided by the generated HSs. The FPs are plotted on an XY -grid formed by d_e, d_i pairs ($X = d_i$ and $Y = d_e$), where the frequencies of occurrence of interactions (the number of points with a given d_e, d_i pair) are represented by different colours. Moreover, the complementary regions are visible in the FPs where one molecule acts as a donor ($d_e > d_i$) and the other as an acceptor ($d_e < d_i$).^{ES5}

Study of intermolecular interactions of compounds 1, 2 and 3 by Hirshfeld surface analysis

The Hirshfeld surfaces mapped with d_{norm} of **1–3** are given in Fig. 1a–c, in which the classical and weak hydrogen bonds are identified with labels.

The features labeled 1 (a deep red area) in Fig. 1a–c are indicative of important interactions in all three structures, *i.e.* $\text{N}_{\text{CP}}\text{--H}\cdots\text{O}_{\text{P}}$ between one phosphoric triamide molecule and its symmetry-related adjacent molecule. It is worth noting that in all three structures only the O atom of $\text{P}=\text{O}$ group takes part in $\text{NH}\cdots\text{O}$ hydrogen bonding.

As mentioned in the section on X-ray crystallography, all three compounds contain weak $\text{CH}\cdots\text{O}$ intermolecular interactions with neighbouring molecules, which are monitored in the

related HS's, as well. In this regard, the red spot marked with label 2 indicates the one remarkable CH...O interaction in the structure **1** (Fig. 1a), while such highlighted CH...O interactions in structures **2** and **3** are introduced by labels 3 and 4 in Fig. 1b and labels 2 and 3 in Fig. 1c. However, the CH...O contacts with lower degrees of importance also appear in the noted HS's maps: labels 3 and 4 in Fig. 1a for **1** and label 4 in Fig. 1c for **3**.

In structure **2**, the very light red spot in Fig. 1b (label 2) is related to the only significant H...H contact which takes place between an H atom of an aromatic ring (C₆H₄) and an H atom of an aliphatic ring (C₆H₁₁). The two other structures do not show such a highlighted H...H interaction. Structure **1**, with the most unsaturated systems with respect to two other structures, reveals weak C...H contacts shown as four small red regions (labels 5–8 in Fig. 1a), formed between the C and H atoms of unsaturated aromatic rings. The other structures do not show such highlighted C...H contacts in related Hirshfeld surfaces.

The full fingerprint plots of compounds **1–3** are illustrated in Figure S 2. These plots represent the total interactions which are also divided into the different types of interactions to show the contribution portion of each contact in the total Hirshfeld surface.

For **1–3**, the H...H interactions, which cover the most surface area of the 2D fingerprint plot, exhibit the most significant contribution to the total Hirshfeld surface with respect to the other contacts (62.6%, 82.2% and 76.6%, respectively in Figs. S3a, S4a and S5a). The very high percentage of H...H interactions in **2** is due to the high number of hydrogen atoms and the bulk groups including hydrogen. A comparison of the H...H contacts in the structure **3** with the previously reported structure [2,6-F₂C₆H₃C(O)NH]P(O)[N(C₂H₅)₂]₂,^{ES6} which is different by two H atoms in **3** instead of two F atoms in the reported structure, reveals that the absence of stronger

H···F interactions allows for a more contributed portion of weaker H···H interactions in the crystal packing of **3** (more about 20%).

Fingerprint plots of S3b, S4b and S5b show O···H contacts in structures **1** to **3**, with two sharp spikes in the regions of the lower and upper sections of the figures. The O···H contacts include both NH···O and CH···O interactions and the highest percentage of O···H contacts was found for the structure **3** (9.4% **1**, 9.5% **2** and 11.5% **3**). The structure **1** with the highest numbers of unsaturated C atoms indicates the highest percentage of weak C···H contacts (26.5%, Figure S 3c). Besides these, there are also contacts with negligible contribution portions in all three structures, such as C···C and O···C, which are not shown in the related fingerprint plots.

IR and NMR Study

Stretching frequencies of the N–H units occur at 3087, 3077 and 3068 cm^{-1} for compounds **1**, **2** and **3**, respectively. The phosphorus chemical shifts of compounds **1**, **2** and **3** are 14.76, 13.77 and 13.09 ppm, respectively.

Table 4 lists the ^1H and ^{13}C NMR assignments of both compounds, with the assignments achieved by 2D experiments. In the ^1H NMR spectra of **1**, **2** and **3**, the broad signals at 9.37, 8.89 and 8.98 ppm, respectively, are related to the corresponding C(O)NHP(O) protons.

The aromatic protons of the $\text{CH}_3\text{--C}_6\text{H}_4\text{C(O)}$ segment in **1–3** are revealed as two doublet signals in the range of 7.78–7.86 ppm for H2 and H6 and 7.26–7.29 ppm for H3 and H5.

In the ^1H NMR spectrum of **1**, the two benzylic protons of the $\text{CH}_2\text{--C}_6\text{H}_5$ section are observed as two dd signals at $\delta = 4.24$ and 4.16 ppm. This pattern is a result of geminal $^2J_{\text{HCH}}$ plus vicinal

$^3J_{\text{PNCH}}$ couplings. The doublet signal at 2.54 ppm ($^3J_{\text{PNCH}} = 10.1$ Hz) is assigned to the N-CH₃ protons.

The H_{axial} and H_{equatorial} signals of the cyclohexyl group in **2** are distinguished by their different splitting patterns. Supported by the Karplus equation^{ES7} and the different P–N–C–H_{axial} and P–N–C–H_{equatorial} torsion angles, the doublet of multiplets at $\delta = 1.74, 1.72, 1.62, 1.59$ and 1.55 ppm are assigned to H_{equatorial} and two *qd* signals at $\delta = 1.50$ and 1.46 ppm and three *qt* at $\delta = 1.22, 1.18$ and 1.02 ppm can be attributed to the H_{axial}. The *tdt* pattern observed at $\delta = 3.31$ ppm is due to the spin coupling between H1' with H_{equatorial} ($^3J_{\text{HCCHeq}} = 11.9$ Hz), H_{axial} ($^3J_{\text{HCCHax}} = 3.5$ Hz) and the phosphorous nuclei ($^3J_{\text{PNCH}} = 9.3$ Hz).

In compound **3**, the *qd* at 3.07 ppm belongs to the CH₂-protons of the N–Et group. This splitting pattern is expected since the distance to ³¹P would yield a doublet signal with $^3J_{\text{PNCH}} = 11.1$ Hz and also, two mutually quartets which are expected from the splitting by the methyl group ($^3J_{\text{HCCH}} = 7.1$ Hz).

For compounds **1–3**, the doublet signals in the ¹³CNMR spectra at $\delta = 168.31, 167.81, 167.82$ ppm (with $^2J_{\text{PC}} = 2.2, 2.2, 2.1$ Hz, respectively) resulting from the coupling with P nuclei, correspond to the C(O) groups. In all three molecules, the doublet signals at $\delta = 130.89$ to 131.28 ($^3J_{\text{PC}}$ in the range of 8.6–8.9 Hz) are assigned to the corresponding C1 atom of CH₃–C₆H₄ segment. It should be noted that each carbon atom of N(CH₃)(CH₂C₆H₅), N(CH₃)(C₆H₁₁) and N(C₂H₅)₂ moieties with two or three bond separations from the corresponding P atom are observed as a doublet signal due to the P–C coupling.

References

ES1. Spackman, M. A.; Byrom, P. G. *Chem. Phys. Lett.* **1997**, 267, 215–220.

- ES2. Hirshfeld, F. L. *Theor. Chim. Acta* **1977**, 44, 129–138.
- ES3. McKinnon, J. J.; Spackman, M. A.; Mitchell, A. S. *Acta Cryst. B* **2004**, 60, 627–668.
- ES4. Spackman, M. A.; Jayatilaka, D. *CrystEngComm* **2009**, 11, 19–32.
- ES5. Spackman, M. A.; McKinnon, J. J. *CrystEngComm* **2002**, 4, 378–392.
- ES6. Tarahhomi, A.; Pourayoubi, M.; Golen, J. A.; Zargaran, P.; Elahi, B.; Rheingold, A. L.;
Leyva Ramírez, M. A.; Mancilla Percino, T. *Acta Cryst. B* **2013**, 69, 260–270.
- ES7. Drago, R. S. *Physical Methods for Chemists*, second ed., Saunders College Publishing,
Florida, **1992**.

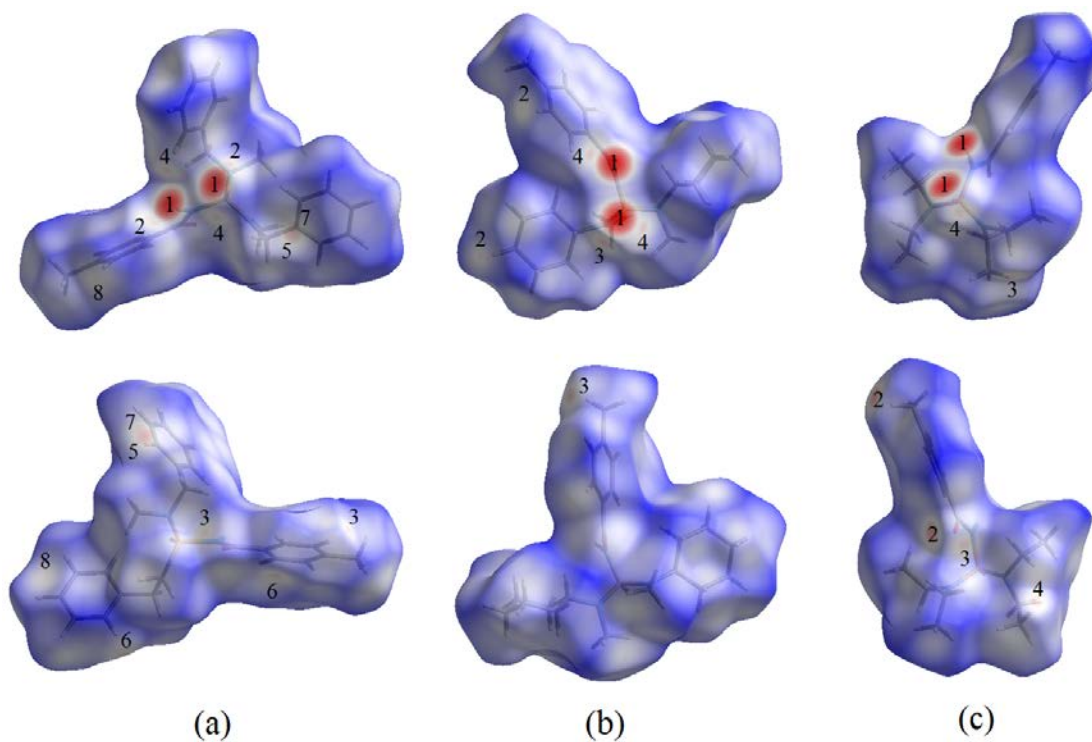


Figure S 1: Two orientations of the Hirshfeld surfaces for molecules **1–3**. Labels on HS's are: (a): NH \cdots O (**1**), CH \cdots O (**2–4**), CH \cdots C (**5–8**); (b): NH \cdots O (**1**), H \cdots H (**2**), CH \cdots O (**3, 4**); (c): NH \cdots O (**1**), CH \cdots O (**2–4**).

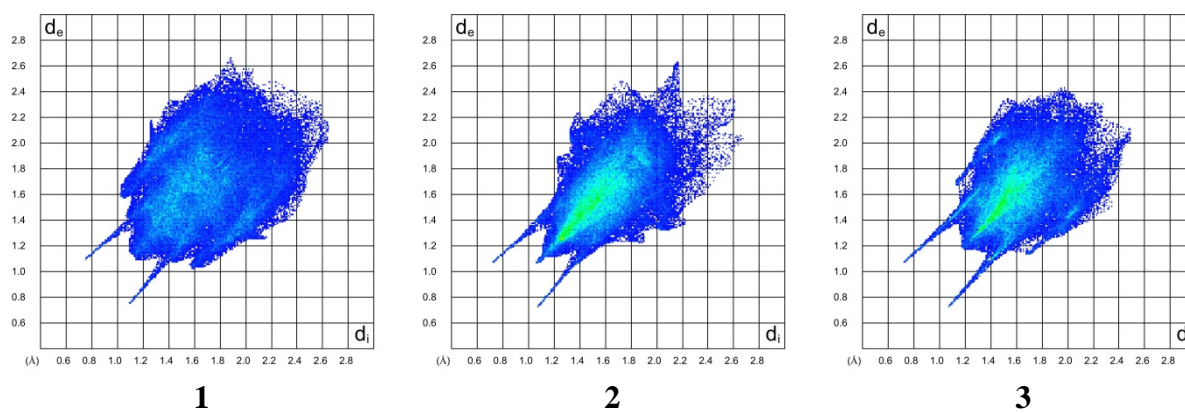


Figure S 2: The full fingerprint plots of compounds **1–3**.

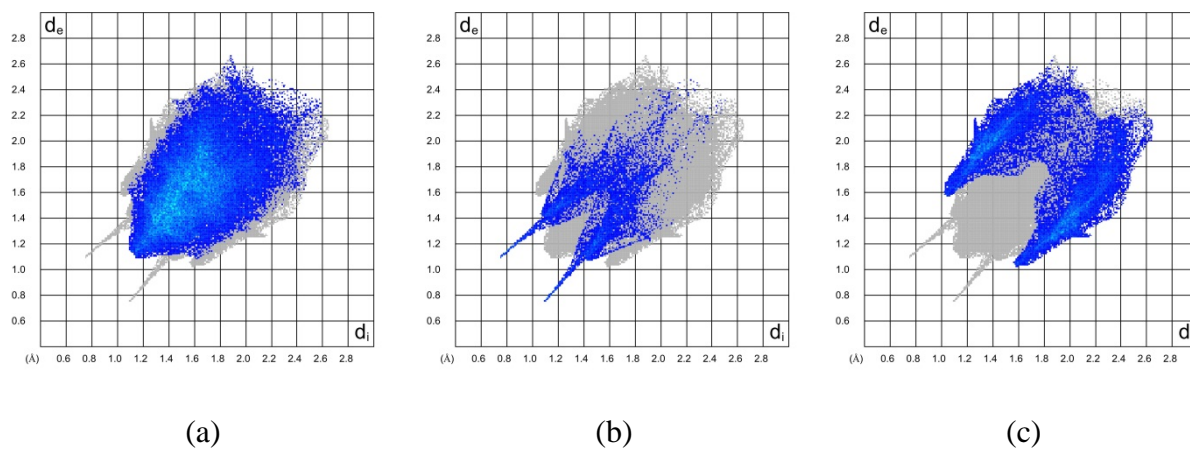


Figure S 3: Divided fingerprint plots for **1**. Close contacts are as follows: (a) H \cdots H (62.6%), (b) O \cdots H / H \cdots O (9.4%) and (c) C \cdots H / H \cdots C (26.5%).

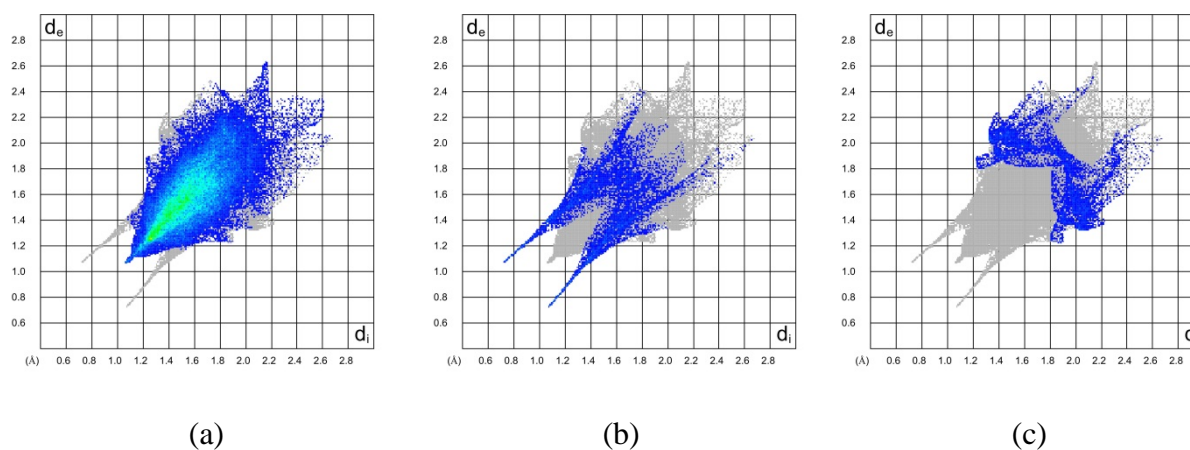


Figure S 4: Divided fingerprint plots for **2**. Close contacts are as follows: (a) H \cdots H (82.2%), (b) O \cdots H / H \cdots O (9.5%) and (c) C \cdots H / H \cdots C (6.4%).

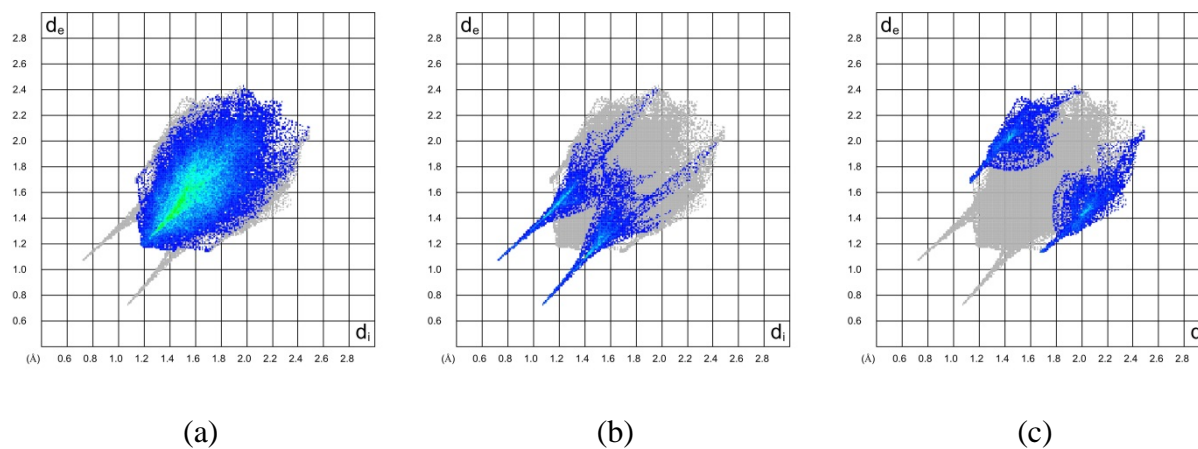


Figure S 5: Divided fingerprint plots for **3**. Close contacts are as follows: (a) H \cdots H (76.6%), (b) O \cdots H / H \cdots O (11.5%) and (c) C \cdots H / H \cdots C (11.8%).

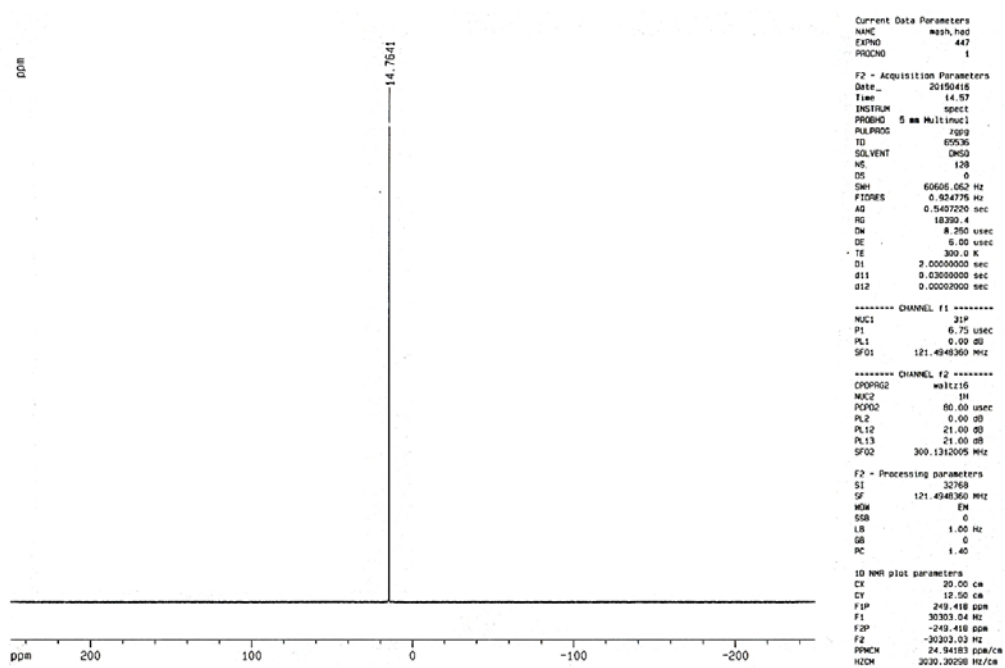


Figure S 6: $^{31}\text{P}\{^1\text{H}\}$ NMR spectrum of compound **1** (DMSO- d_6).

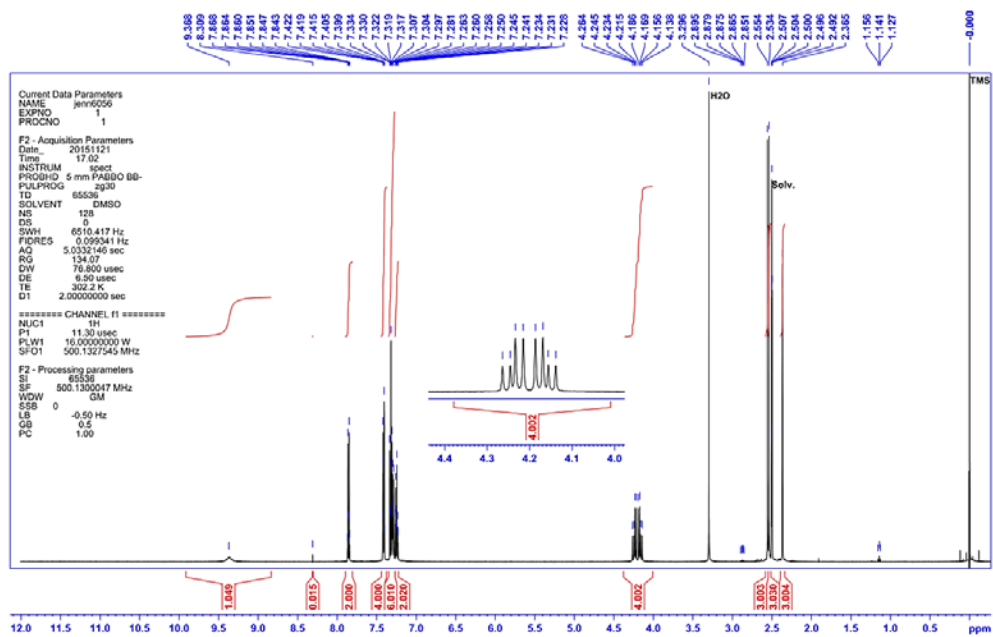


Figure S 7: ^1H NMR spectrum of compound 1 (DMSO- d_6).

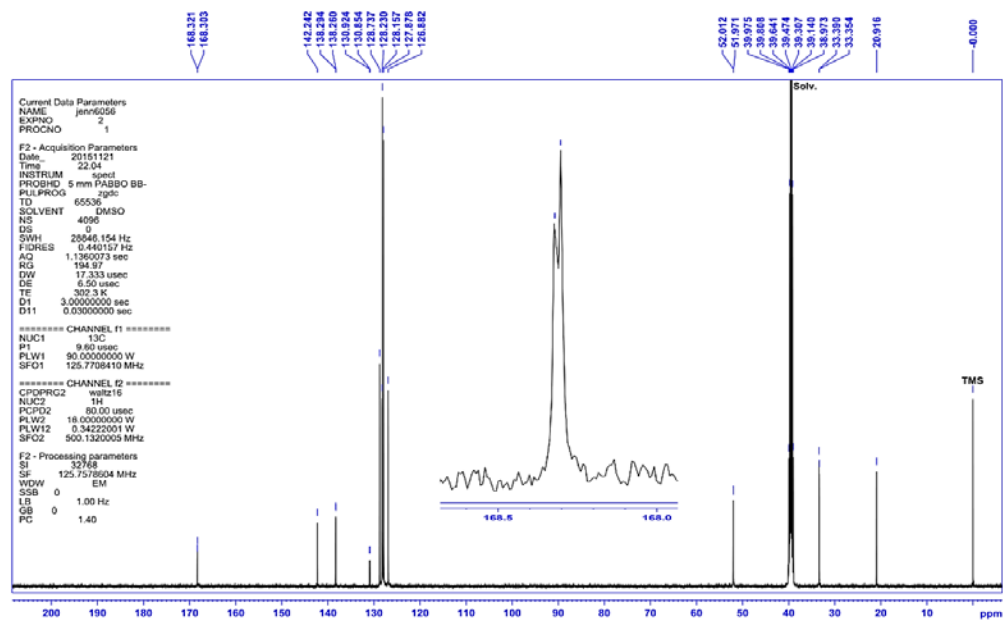


Figure S 8: ^{13}C NMR spectrum of compound 1 (DMSO- d_6).

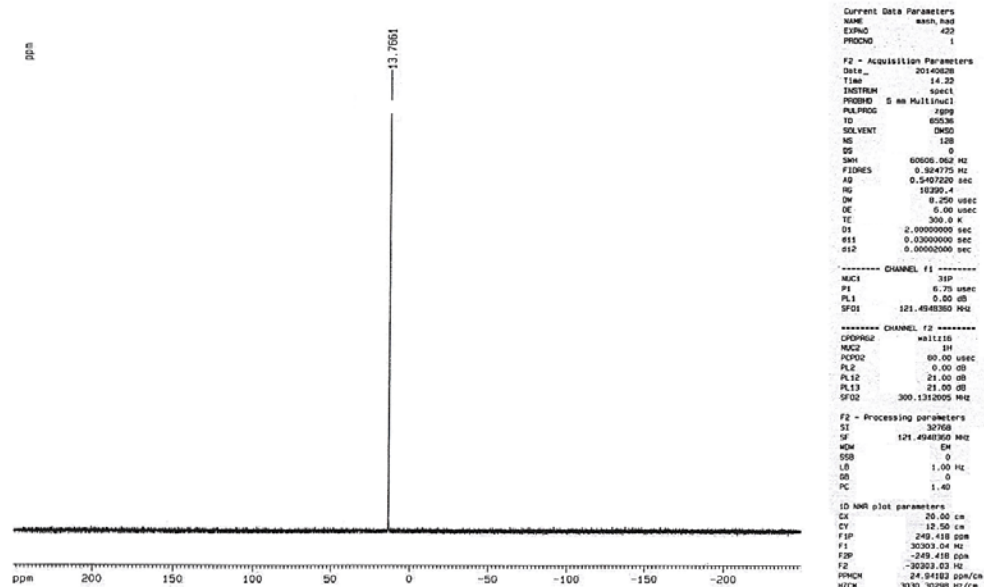


Figure S 9: $^{31}\text{P}\{^1\text{H}\}$ NMR spectrum of compound 2 (DMSO- d_6).

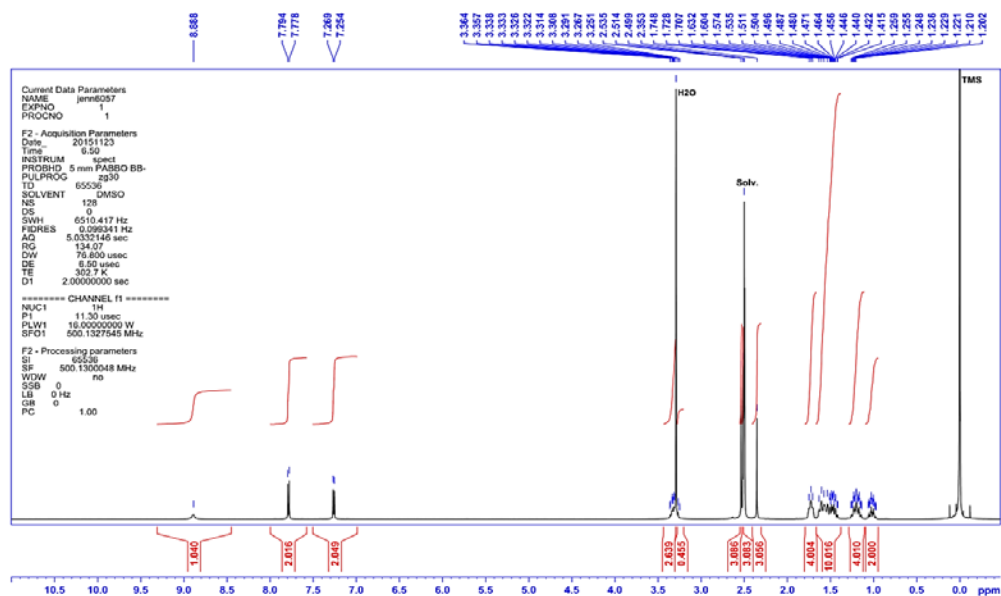


Figure S 10: ^1H NMR spectrum of compound 2 (DMSO- d_6).

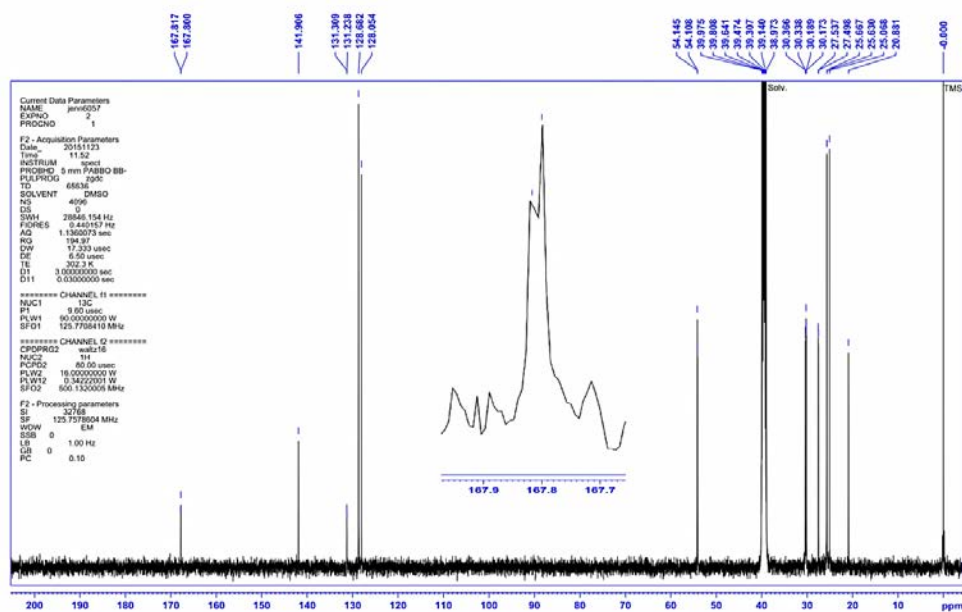


Figure S 11: ^{13}C NMR spectrum of compound 2 (DMSO- d_6).

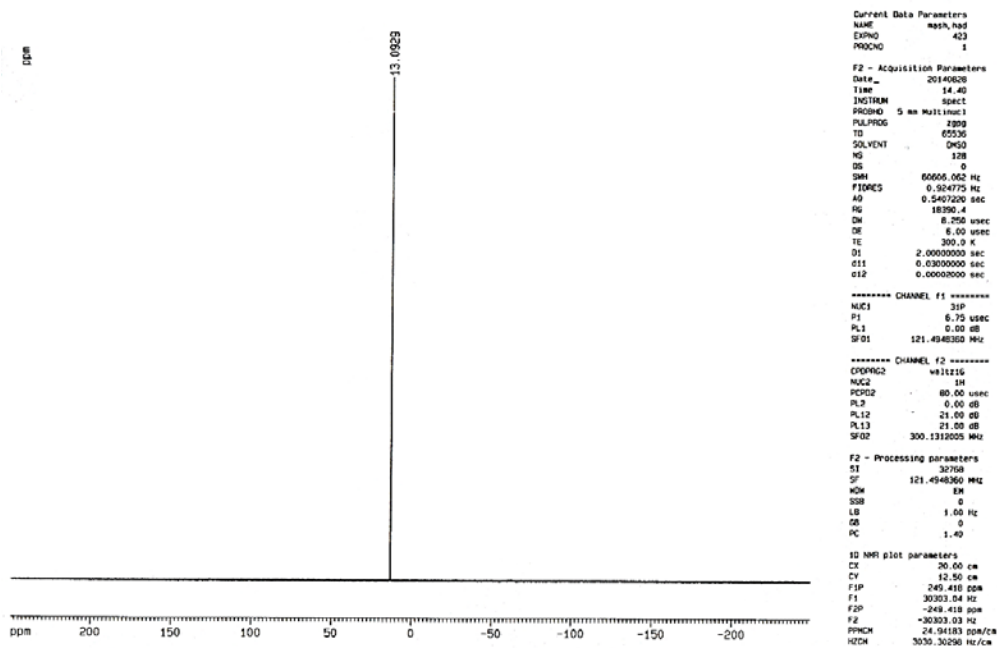


Figure S 12: $^{31}\text{P}\{^1\text{H}\}$ NMR spectrum of compound 3 (DMSO- d_6).

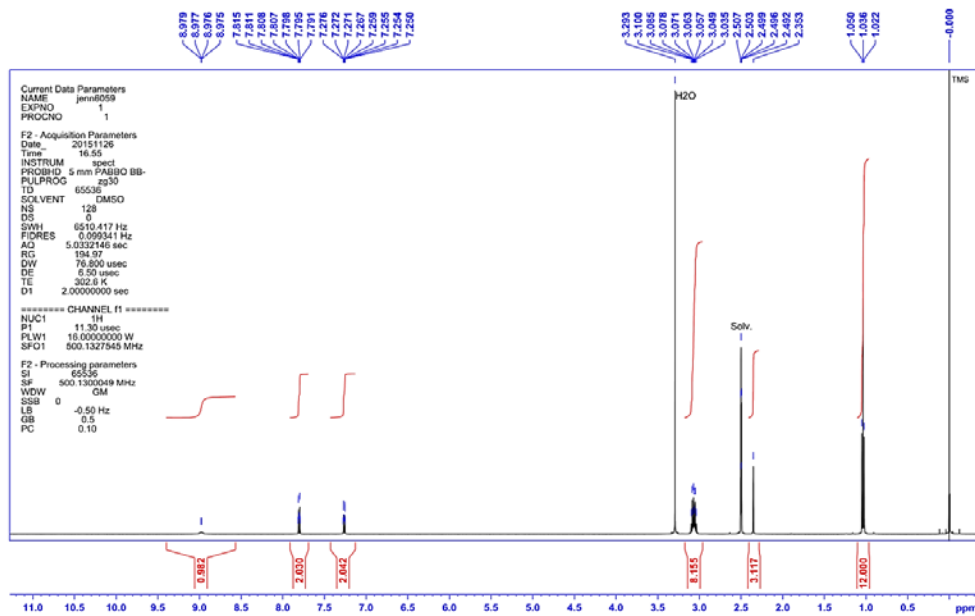


Figure S 13: ^1H NMR spectrum of compound **3** ($\text{DMSO}-d_6$).

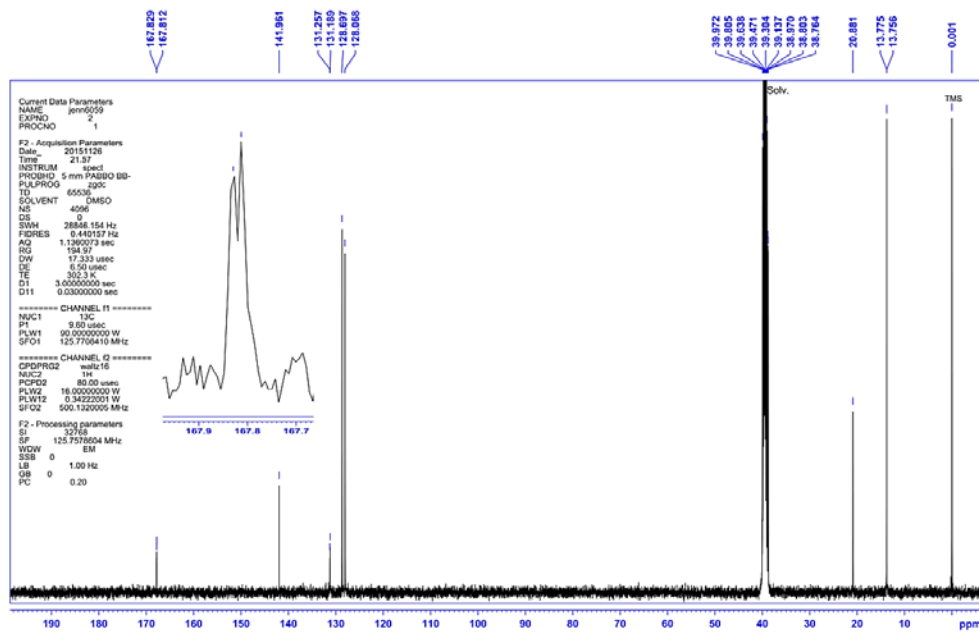


Figure S 14: ^{13}C NMR spectrum of compound **3** ($\text{DMSO}-d_6$).